JOURNAL OF MAGNETIC RESONANCE, 29, 433–462 (1978)

Selective Excitation in Fourier Transform Nuclear Magnetic Resonance

GARETH A. MORRIS AND RAY FREEMAN

Physical Chemistry Laboratory, University of Oxford, South Parks Road, Oxford, England

Received July 12, 1977

The applications of frequency-selective excitation methods in Fourier transform NMR are discussed, and a simple technique is described for selective excitation of a narrow frequency region of a high-resolution NMR spectrum in a Fourier transform spectrometer. A regular sequence of identical radiofrequency pulses of small flip angle exerts a strong cumulative effect on magnetizations close to resonance with the transmitter frequency or one of a set of equally spaced sidebands separated by the pulse repetition rate. All other magnetizations precess through an incomplete number of full rotations between pulses, and are caught by successive pulses at an ever changing phase of their precession, which destroys the cumulative effect. The motion of the various nuclear magnetization vectors may be described pictorially according to the Bloch equations, neglecting relaxation during the pulse sequence. A general theory is presented for selective or "tailored" excitation by an arbitrary modulation of the radiofrequency transmitter signal. It confirms earlier conclusions that the frequency-domain excitation spectrum corresponds to the Fourier transform of the transmitter modulation pattern, provided that the NMR response remains linear. The excitation spectra calculated for the selective pulse sequence by these two alternative approaches show good agreement within their respective limitations. A number of practical applications of selective excitation are explored, including solvent peak suppression, the detection of partial spectra from individual chemical sites, selective studies of relaxation and slow chemical exchange, and hole-burning or localized saturation.

1. INTRODUCTION

1.1. Applications of Selective Excitation

Most modern NMR spectrometers for high-resolution work operate in the Fourier transform mode in which the excitation is produced by strong nonselective radiofrequency pulses. In this fashion an important improvement in sensitivity is achieved, transient phenomena such as relaxation may easily be followed, and a good approximation to the slow-passage linewidth is obtained. The majority of the applications of the Fourier transform method have no need for linear sweep or fine adjustment of the transmitter frequency, and such facilities are not normally provided in dedicated Fourier spectrometers. There are, however, a number of experiments in which fine adjustment and selectivity in the frequency domain would be a decided advantage.

The most widely encountered problem is that created by intense solvent resonances (particularly water) which make excessive demands on receiver linearity and on the

0022–2364/78/0293–0433$02.00/0

DOI of original item: doi: 10.1016/0022-2364(78)90003-3

dynamic range of the analog-to-digital converter. Several of the methods suggested for solvent peak suppression involve selective irradiation, either to saturate the solvent resonance (*1–11*) or to avoid exciting it (*12–15*). One of the principal advantages claimed for the new technique of correlation spectroscopy (*16–18*) is this ability to examine a spectrum without allowing the transmitter frequency to sweep through the strong solvent line.

A severe limitation on the applicability of NMR to large molecules is the complexity that results from the crowding together of many overlapping spin multiplets. This problem has provided the impetus for the development of very high field superconducting solenoids for the study of biologically significant systems. The growing interest in proton-coupled carbon-13 spectra (*20–26*) provides an illustration of this problem, since even in relatively simple molecules there can be severe overlap of spin multiplets. Frequently this can be the most important factor limiting the size of molecule which may be studied. When heteronuclear spin coupling is responsible for the overlap problem, selective excitation methods can provide a solution.

Wideband proton irradiation collapses the multiplet structure of carbon-13 spectra, giving a significant sensitivity improvement at the expense of the loss of all proton–carbon coupling information. This means that carbon-13 chemical shifts are available after relatively short periods of signal averaging. Knowledge of the chemical shifts makes it possible to unravel complex proton-coupled spectra by a simple combination of selective excitation and gated decoupling (*27–30*). The carbon-13 multiplets are collapsed by proton irradiation, leaving one resonance for each chemically distinct site. One such resonance is excited selectively, and the decoupler is then switched off to allow free precession under proton-coupled conditions. Fourier transformation of the resultant free-induction decay generates a multiplet "subspectrum" corresponding to the chosen carbon site. A series of such subspectra may be assembled, one for each chemical shift frequency; their sum is just the normal full proton-coupled spectrum. The effect of the sequence of experiments is to decompose the spectrum into its components, revealing in full all the information previously obscured by overlap.

This technique is clearly applicable to multiplet structure that is partly dipolar in origin, as in spectra of partially oriented molecules in a liquid-crystal phase. Excitation of partial spectra in this fashion can also be important when very high resolution is required over a relatively narrow spectral region, for it permits very fine digitization to be used in the frequency domain without introducing aliasing problems (*30*).

Additional information about proton-coupled carbon-13 multiplets may be obtained by selective pulsed double-resonance techniques, such as selective population transfer (*31–39*). These methods allow the relative signs of proton–carbon coupling constants to be determined using "soft" selective pulses in the proton spectrum. The analogous experiments are well known in proton magnetic resonance (*40*). Selective irradiation is also important in the study of chemical exchange processes by following the transfer of saturated magnetization, first proposed by Forsén and Hoffman (*41–44*).

The study of relaxation mechanisms is another field where the pulse sequence used to perturb the spin system may be required to be frequency selective (*45–59*). Cross-relaxation effects in the spin–lattice relaxation of protons may be studied by comparing the recovery after a selective population inversion pulse with the recovery after a completely nonselective pulse (*60–65*). The analysis is particularly simple if only the initial rates are considered. More detailed insight into cross-relaxation is obtained if the

relaxation after multiple selective population inversions is studied. Information on molecular structure and dynamics is available from such experiments.

The determination of spin–spin relaxation times in the presence of homonuclear spin–spin coupling by spin echo methods is greatly hampered by J modulation of the echoes (*66–69*). This modulation normally disappears if the chemically shifted groups are examined individually by means of a pulse sequence in which excitation and refocusing pulses are frequency selective (*69*).

Spin locking, or forced transitory precession (*70–77*), is an attractive alternative method for studying spin–spin relaxation in liquids, avoiding the modulation effects encountered with spin echoes. Since the spin-locking radiofrequency field must be applied for times comparable with the spin–spin relaxation time T_2, and must be strong compared with the range of chemical shifts to be studied, considerable problems with radiofrequency heating of the sample arise. This difficulty is circumvented if a frequency-selective experiment is performed, exciting the chemically shifted spin multiplets one at a time, with a radiofrequency field strong compared with the multiplet splitting but weak compared with the chemical shift difference of the nearest group (*46*, *77*).

Finally there are some important experiments that require the radiofrequency excitation to be restricted to certain geometrical regions of the sample. One such technique is that of spin mapping (*78–84*) or zeugmatography (*85–89*), the determination of the density of nuclei (usually protons in water) inside an object as a function of the spatial coordinates, by examining the NMR signals in the presence of strong applied static field gradients. Several such methods (*80*, *84*) use selective irradiation schemes to saturate or excite selected small regions of the sample. Variation of the irradiation frequency or the magnetic field gradients allows the coordinates of this chosen region to be scanned, thus mapping out the spin density within the sample. The speed with which the selective pulse sequence can be computed is a critical factor in the attainable sensitivity of one embodiment of this experiment (*84*) and for this purpose a simplified sequence would be preferable to the full synthesized excitation technique of Tomlinson and Hill (*14*).

A related technique in the field of high-resolution NMR would be to restrict the effective sample volume by selective excitation in both natural field gradients and superimposed strong applied gradients. The nuclear spin response would be monitored with the imposed gradients removed. If the imposed gradients are chosen so as to match the dominant natural gradients, the sample region excited would correspond to a highly homogeneous field, and the signal from this region would transform to a spectrum where the linewidths were significantly narrower than the normal instrumental width. An equivalent physical reduction in the *actual* size of the sample is not usually possible since the shape and location of the region of high homogeneity are not known, and because of bulk susceptibility changes at the sample boundaries. These experiments are related to localized saturation, or "hole burning" (*90–92*), which has been used for precise measurement of frequency separations in high-resolution double resonance (*91*) and for approximate measurements of natural linewidths (*92*).

1.2. Methods of Selective Excitation

One of the first techniques used to excite a chosen resonance with a pulse while avoiding excitation of a nearby resonance was proposed for spin echo work by

Alexander (*12*). The principle is to use a relatively weak pulse of long duration, calculated to give a 90° flip to the chosen resonance line, but a 360° flip to the neighboring line, which experiences an effective field in the rotating frame $H_{\text{eff}} = 4H_1$. Redfield (*13*) has extended this idea to solvent peak suppression in Fourier transform NMR, using a computer to calculate the corrections for the phase and intensity distortions inherent in this method.

For spectra with well-resolved groups of resonance lines, a simpler weak-pulse method may be employed. The radiofrequency intensity is set so low that only the chosen group of lines is affected significantly, while all other groups are so far from resonance ($\Delta H \gg H_1$) that their excitation is negligible (*45–59*). In the limit of extremely weak pulses, it is possible to pick out one component line of a spin multiplet for excitation (*46*). These techniques were developed on conventional "continuous-wave" spectrometers with facilities for fine adjustment of the irradiation frequency; modern Fourier transform spectrometers do not normally have this capability.

For Fourier transform spectrometers Tomlinson and Hill (*14*) have proposed a very general method in which the frequency spectrum of the excitation may be "tailored" to any desired pattern. The operator simply defines the desired excitation spectrum in the frequency domain, and the computer calculates the Fourier transform of this pattern and uses it to modulate the amplitude or the pulse width of a sequence of radiofrequency pulses. This "synthesized excitation" technique has been applied successfully to solvent peak suppression (*14*), transient and steady-state nuclear Overhauser effects (*53*), selective spin locking (*77*), and spin mapping(*84*). It remains the most versatile general method of selective excitation proposed to date, but it does have some drawbacks. The very generality of the frequency-domain excitation pattern requires that considerable computer storage be set aside to retain this information, typically halving the data space available for NMR signals. Furthermore, the provision of a pulse modulation scheme that has the required linearity is by no means trivial. Amplitude modulation requires that the radiofrequency amplifier and probe response be linear, whereas conventional transmitters use "Class C" amplifiers and nonlinear probe networks to achieve good isolation between transmitter and receiver. Linear pulse width modulation is difficult to implement since the probe "Q" factor limits the minimum pulse width that can be employed (*93*). The price paid for versatility is a considerable increase in instrumental complexity.

However, a critical examination of applications of selective excitation suggests that complex excitation patterns are seldom needed, for the majority of experiments could be carried out with one (or perhaps two) effectively monochromatic irradiation fields. In conjunction with conventional nonselective pulses and radiofrequency phase inversion, it should be possible to perform the majority of selective excitation experiments without recourse to synthesized excitation. This "effectively monochromatic" irradiation, finely adjustable in frequency, can be achieved in an extremely simple manner with the minimum modification to a conventional Fourier transform spectrometer (*28*). This selective pulse sequence consists of a regular train of identical, short, strong radiofrequency pulses, each with flip angle $\alpha \ll \pi/2$ radians, spaced τ sec apart. Only those resonances that are offset from the transmitter by $\Delta\nu = n/\tau$ Hz, where n is an integer, are excited to a significant extent. The nature of this selectivity is examined in more detail in the next section, but a number of useful results may be derived relatively simply.

Fourier analysis of the pulse sequence shows that if the pulse widths Δt are much less than the pulse interval τ, then the selective pulse sequence is approximately equivalent to the superposition of a number of continuous radiofrequency signals with frequencies spaced $1/\tau$ Hz apart, which can be regarded as "sidebands" symmetrically disposed with respect to the transmitter frequency at ν_0, $\nu_0 \pm 1/\tau$, $\nu_0 \pm 2/\tau$, etc., each of amplitude $H_1\Delta t/(\Delta t + \tau)$, where H_1 is the pulse amplitude. For a magnetization close to one of these sideband conditions, the pulse sequence acts just like a weak selective pulse. A suitable choice of transmitter frequency ν_0 and repetition rate $1/\tau$ will ensure that only one sideband (normally the first sideband at $\nu_0 \pm 1/\tau$) falls within the spectrum of interest. For nuclear magnetization components that are not in the immediate vicinity of one of the sidebands, the influence of the next-nearest sideband must also be taken into account and this simple picture breaks down. This situation has been treated for slow-passage NMR by Bloch and Siegert (*94*) and Ramsey (*95*).

A more pictorial description of the effects of the selective pulse sequence may be obtained by following the motion of a macroscopic magnetization vector **M** at a frequency offset $\Delta\nu$ Hz from the transmitter. Each pulse nutates **M** through α radians about the X axis of the rotating frame, while each pulse interval allows **M** to precess about the Z axis through $2\pi\Delta\nu\tau$ radians. If relaxation can be neglected during the relatively short total duration of the sequence, the motion is composed only of alternate rotations about the X and Z axes. It is readily seen that if **M** precesses through an integral number of complete revolutions during the interval τ, successive pulses will find **M** in the YZ plane and their overall effect will be a cumulative rotation about the X axis in a number of small steps. This is the same effect as that of a weak field on resonance, the conditions $2\pi\Delta\nu\tau = 2\pi n$ corresponding to the sideband condition $\Delta\nu = n/\tau$ described above. This condition achieves the maximum excitation.

A magnetization at a more general offset $\Delta\nu = (2n\pi + \theta)/2\pi\tau$, will precess through an excess angle θ in each pulse interval, being carried progressively further away from the YZ plane, which robs the pulses of their full cumulative effect. The fate of such components is readily illustrated by computer simulations based on the Bloch equations, neglecting relaxation. Figure 1 shows a family of such trajectories calculated for a sequence of 20 pulses with flip angle $\alpha = \pi/40$ radians and pulse interval 2 msec. The "first sideband" condition is thus $\Delta\nu = 500$ Hz, and the frame of reference is chosen to rotate at $\nu_0 + 500$ Hz, in synchronism with the first sideband. The advantage of this particular rotating frame is that the family of magnetization vectors then precesses through only small "excess" angles θ between pulses, simplifying the trajectories. The vector for $\Delta\nu = 500$ Hz then remains throughout in the YZ plane, so that after twenty pulses it has rotated from the Z axis to the Y axis, corresponding to a perfect selective 90° pulse. Vectors only a few hertz away from this condition are curled away from the YZ plane, while vectors greater than 25 Hz distant execute small approximately circular trajectories near the Z axis, never having a significant component along the X or the Y axis of the rotating frame.

These calculations can be extended to illustrate how the X component (dispersion) and Y component (absorption) of a magnetization **M** at the end of the sequence depend on the offset from the transmitter frequency ν_0 (Fig. 2). The scale has been normalized with respect to the equilibrium magnetization M_0, so that a 90° pulse at the exact sideband condition gives a transverse signal of unit intensity. Such diagrams may be

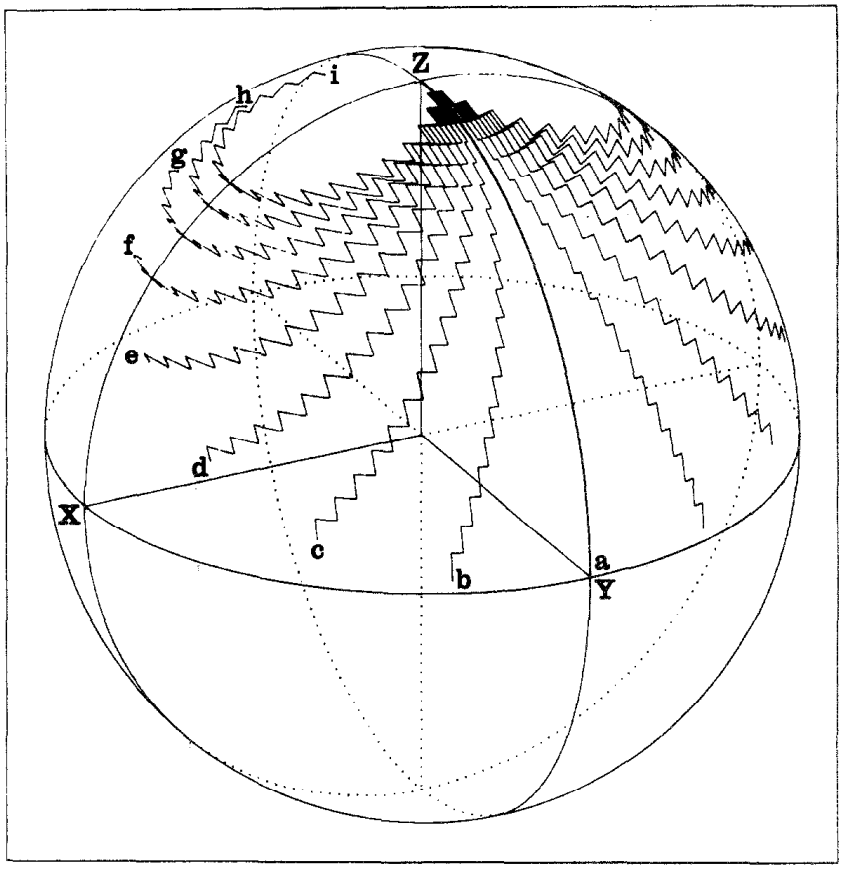

FIG. 1. Trajectories of magnetization vectors computed according to the Bloch equations and viewed in a frame of reference rotating at the "first sideband" frequency, $\nu_0 + 500$ Hz. The excitation was a train of twenty pulses of flip angle $\pi/40$ radians each, spaced 2 msec apart. Trajectory (a) represents magnetization exactly 500 Hz above the transmitter frequency ν_0 and it experiences a cumulative nutation of $\pi/2$ radians with no net precession between pulses. Trajectories (b) through (i) represent increasing offsets in steps of 2.5 Hz up to a total of 520 Hz above ν_0, the unlabeled trajectories representing the corresponding offsets below 500 Hz.

termed "excitation spectra." The weak oscillations in the flanks of the main excitation peak reflect the cyclic excursions noted in Fig. 1. It will be seen later that these excitation spectra are very similar to those obtained by Fourier transformation of the pulse sequence.

1.3. Nomenclature

In the search for a suitable name for the selective pulse sequence, a striking literary parallel with the type of magnetization trajectory discussed in Section 1.2 was discovered. The second section of Dante Alighieri's "La Divina Commedia," the "Purgatorio," describes a journey through Purgatory by Dante and Virgil. Dante's Purgatory consists of a series of ten circular ledges, one above the other, running around a mountain. Souls in Purgatory progress toward Heaven by circumnavigating each ledge before moving up to the next. This motion is the exact reverse of that undergone by the tip of a magnetization vector close to the first sideband condition of a ten-pulse selective pulse sequence, when viewed in a frame of reference rotating at the

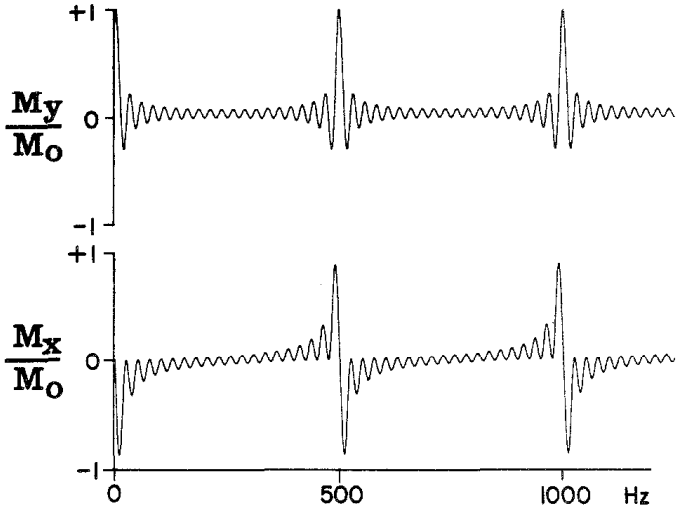

FIG. 2. Frequency-domain excitation spectra corresponding to the pulse sequence used in Fig. 1, showing the Y and X components of magnetization immediately after the last pulse of a selective pulse sequence as a function of the offset from the transmitter frequency. The computer simulation was based on the Bloch equations, neglecting relaxation. Note that the number of weak maxima between the main excitation peaks of M_y is given by m-2, where m is the number of pulses in the sequence.

transmitter frequency. The selective pulse sequence has thus acquired the name DANTE (Delays Alternating with Nutations for Tailored Excitation). A similar relationship has led to the naming of the spin-locking experiments to be described in Sections 2.3 and 3.5 after Dante's Inferno, which has the form of a cone whose apex lies at the center of the earth. The trajectory of a magnetization during an INFERNO experiment (Irradiation of Narrow Frequency Envelopes by Repeated Nutation and Orbiting) lies on the surface of just such a cone (see Fig. 8).

2. THEORY OF SELECTIVE EXCITATION

2.1. General Treatment for an Arbitrary Excitation

The problem of calculating the frequency dependence of the effects of a completely general radiofrequency perturbation $H_1(t)$ may be attacked in one of two basic ways. The first is to use the Bloch equations in the time domain to give an explicit solution for each individual frequency. This becomes progressively more difficult as $H_1(t)$ becomes more complicated, but for excitation methods such as the DANTE pulse sequence it can provide useful insights. It is difficult to derive analytical results in the time domain, and hence computer methods are required to produce quantitative excitation spectra.

The second approach is to solve the problem in the frequency domain. Provided the response of the spin system remains approximately linear, the excitation spectrum of a perturbation $H_1(t)$ will be proportional to its Fourier transform. This result, much used in linear system theory, greatly facilitates the analytical treatment of selective excitation, and provides a ready conceptual link between the form of a pulse sequence and its excitation spectrum.

The concepts of Fourier transformation have been widely used in magnetic resonance (see, for example, Ref. (*2*, *13*, *47*, *97–101*)), but do not appear to have been used in an analytical treatment of transient selective excitation. Various analyses of the steady-

state response to repetitive pulse sequences have been performed by other methods (*102–105*). Despite the fact that pulse Fourier transform spectrometers routinely operate in a nonlinear region of the spin response, considerable insight into frequency-selective effects may be achieved by examining the linear response.

The most convenient starting point for a consideration of the selectivity that may be achieved in the frequency domain is the set of phenomenological equations of Bloch (*106*) which describe magnetic resonance effects in terms of magnetization vectors, or isochromats, $\mathbf{M}(\Delta\omega)$. The response to a short "hard" radiofrequency pulse of flip angle α at time $t = 0$ may be described in terms of the magnetization components immediately before the pulse, M_x^-, M_y^-, and M_z^-. The transient solution of the Bloch equations is then

$$M_z(t) = M_z^- \cos\alpha - M_y^- \sin\alpha + M_0\,[1 - \exp(-t/T_1)], \quad [1]$$

$$M_y(t) = (M_y^- \cos\alpha\cos\Delta\omega t + M_z^- \sin\alpha\cos\Delta\omega t - M_x^- \sin\Delta\omega t)\exp(-t/T_2), \quad [2]$$

$$M_x(t) = (M_x^- \cos\Delta\omega t + M_y^- \cos\alpha\sin\Delta\omega t + M_z^- \sin\alpha\sin\Delta\omega t)\exp(-t/T_2). \quad [3]$$

If it can be assumed that $\mathbf{M}$ remains close to the Z axis of the rotating reference frame, so that $M_z \simeq M_0$, and that the flip angle α is small, so that $\sin\alpha \simeq \alpha$ and $\cos\alpha \simeq 1$, then Eqs. [1]–[3] reduce to

$$M_z(t) = M_0, \quad [4]$$

$$M_y(t) = (M_y^- \cos\Delta\omega t + M_0\,\alpha\cos\Delta\omega t - M_x^- \sin\Delta\omega t)\exp(-t/T_2), \quad [5]$$

$$M_x(t) = (M_x^- \cos\Delta\omega t + M_y^- \sin\Delta\omega t + M_0\,\alpha\sin\Delta\omega t)\exp(-t/T_2). \quad [6]$$

This impulse response may be written in terms of the complex transverse magnetization, $M_{xy}(t)$:

$$M_{xy}(t) = M_x(t) + iM_y(t) = (M_{xy}^- + iM_0\,\alpha)\exp(-t/T_2)\exp(-i\Delta\omega t). \quad [7]$$

An isochromat initially at thermal equilibrium subjected to a regular sequence of m short hard pulses of flip angle α_n at times t_n will generate transverse magnetization at the end of the sequence ($t > t_m$) given by the expression

$$\begin{aligned} M_{xy}(t) = \{&\alpha_m + \alpha_{m-1}\mathbf{exp}[-(t_m - t_{m-1})/T_2]\mathbf{exp}[-i\Delta\omega\,(t_m - t_{m-1})] \\ &+ \cdots + \alpha_1\mathbf{exp}[-(t_m - t_1)/T_2]\mathbf{exp}[-i\Delta\omega(t_m - t_1)]\}iM_0\mathbf{exp}[-(t - t_m)/T_2] \\ &\mathbf{exp}[-i\Delta\omega(t - t_m)], \end{aligned} \quad [8]$$

where the operator **exp** is defined by

$$\mathbf{exp}(x) = e^x \qquad \text{for } x < 0,$$

$$\mathbf{exp}(x) = 0 \qquad \text{for } x > 0.$$

Expression [8] simplifies to

$$M_{xy}(t) = iM_0 \sum_{n=1}^{m} \alpha_n\,\mathbf{exp}\,[-(t - t_n)/T_2]\,\mathbf{exp}\,[-i\Delta\omega(t - t_n)]. \quad [9]$$

It is possible to write this in terms of the convolution operation, defined as

$$f(x) \otimes g(x) = \int_{-\infty}^{\infty} f(x')\, g(x - x')\, dx',$$

$$M_{xy}(t) = iM_0 \left\{ \sum_{n=1}^{m} \alpha_n \delta(t - t_n) \right\} \otimes \mathbf{exp}\ (-t/T_2)\ \mathbf{exp}\ (-i\Delta\omega t). \qquad [10]$$

This is an example of a general class of results in linear systems theory, linking the response $R(t)$ to the excitation $E(t)$ by means of the impulse response $h(t)$

$$R(t) = E(t) \otimes h(t). \qquad [11]$$

Equation [10] may be converted into an expression of the form of Eq. [11] by considering a complex radiofrequency excitation $H_1(t)\cos\omega_0 t$, where ω_0 is the angular frequency of the rotating frame of reference. In this frame the perturbing field is $H_1(t)$; it is considered to be composed of an infinite number of impulses dt sec long, so that the impulse corresponding to time t' has a flip angle $\alpha(t') = \gamma H_1(t')dt$. Conversion of the summation in Eq. [10] into an integral gives

$$M_{xy}(t) = iM_0 \int_{-\infty}^{t} \gamma H_1(t')\, \delta(t - t') \otimes \mathbf{exp}\ (-t/T_2)\ \mathbf{exp}\ (-i\Delta\omega t)\, dt'$$

$$= iM_0\, \gamma H_1(t) \otimes \mathbf{exp}\ (-t/T_2)\ \mathbf{exp}\ (-i\Delta\omega t). \qquad [12]$$

In this way the transverse magnetization $M_{xy}(t)$ resulting from an excitation $H_1(t)$ has been expressed in the general form of Eq. [11].

Equation [12] is a simple expression for the transverse magnetization due to an isochromat **M** of frequency $\Delta\omega$ in the rotating frame, as a function of time. It may be expressed as a function of frequency $M_{xy}(\Delta\omega)$ at a particular time t_1 by Fourier transformation of the right-hand side of Eq. [12], using the identity

$$f(0) = \frac{1}{2\pi} \int_{-\infty}^{+\infty} \mathrm{FT}^{-}[f(t)]\, d\omega, \qquad [13]$$

where FT^{-} indicates the Fourier transform operation, and FT^{+} the inverse Fourier transformation (*107*, *108*). This gives for the transverse magnetization at time t_1

$$M_{xy}(\Delta\omega) = \frac{i\gamma}{2\pi} M_0(\Delta\omega) \int_{-\infty}^{+\infty} \mathrm{FT}^{-}[H_1(t - t_1) \otimes \mathbf{exp}\ (-t/T_2)\ \mathbf{exp}\ (-i\Delta\omega t)]\, d\omega. \qquad [14]$$

This permits the convolution theorem (*107*, *108*) to be used to separate the two functions on the right-hand side of Eq. [12]

$$M_{xy}(\Delta\omega) = \frac{i\gamma}{2\pi} M_0(\Delta\omega) \int_{-\infty}^{+\infty} \mathrm{FT}^{-}[H_1(t - t_1)]\ \mathrm{FT}^{-}[\mathbf{exp}\ (-t/T_2)\ \mathbf{exp}\ (-i\Delta\omega t)]\, d\omega. \qquad [15]$$

This may be expanded in terms of standard transforms to give

$$M_{xy}(\Delta\omega) = \frac{i\gamma}{2\pi} M_0(\Delta\omega) \int_{-\infty}^{+\infty} \mathrm{FT}^{-}[H_1(t - t_1)]\, [A(\omega) \otimes \delta(\omega + \Delta\omega)]\, d\omega, \qquad [16]$$

where $A(\omega)$ has been written for the complex Lorentzian

$$A(\omega) = (T_2 - i\omega T_2^2)/(1 + \omega^2 T_2^2). \quad [17]$$

Equation [16] may be rearranged by making use of the identity, easily proved by writing the convolution explicitly and changing the order of integration.

$$\int_{-\infty}^{+\infty} a(\omega)[b(\omega) \otimes c(\omega)]\, d\omega = \int_{-\infty}^{+\infty} [a(\omega) \otimes b(-\omega)]\, c(\omega)\, d\omega, \quad [18]$$

with the result

$$M_{xy}(\Delta\omega) = \frac{i\gamma}{2\pi} M_0(\Delta\omega) \int_{-\infty}^{+\infty} \{\mathrm{FT}^-[H_1(t - t_1)] \otimes A(-\omega)\}\, \delta(\omega + \Delta\omega)\, d\omega. \quad [19]$$

This may be simplified by means of the integral representation of the δ function:

$$M_{xy}(\Delta\omega) = (i\gamma/2\pi) M_0(\Delta\omega) \{\mathrm{FT}^-[H_1(t - t_1)] \otimes A(\omega)\}_{\omega=\Delta\omega}. \quad [20]$$

If an excitation spectrum $E(\Delta\omega)$ is defined such that

$$E(\Delta\omega) = (i\gamma/2\pi)\, \mathrm{FT}^-\, [H_1(t - t_1)] \otimes A(\omega), \quad [21]$$

then Eqs. [20] and [21] may be simply written:

$$M_{xy}(\Delta\omega) = M_0(\Delta\omega)\, E(\Delta\omega). \quad [22]$$

If relaxation can be neglected during the period of application of the excitation $H_1(t)$, this leads to a particularly simple result. The transverse magnetization generated from an isochromat at a frequency $\Delta\omega$ is directly proportional to the Fourier component of the excitation $H_1(t)$ at that frequency:

$$M_{xy}(\Delta\omega) = i\gamma M_0(\Delta\omega)\, \mathrm{FT}^-[H_1(t - t_1)]. \quad [23]$$

Thus the excitation of a spin system as a function of frequency is simply proportional to the Fourier transform of the radiofrequency excitation, provided that the excitation time is short compared to the relaxation times T_1 and T_2, and that the net perturbation at any frequency is small.

Equation [23] may be inverted to produce the pulse sequence necessary for a desired excitation spectrum $E(\Delta\omega)$:

$$H_1(t - t_1) = (1/i\gamma)\, \mathrm{FT}^+[E(\Delta\omega)]. \quad [24]$$

This is the basis of the "synthesized excitation" experiment of Tomlinson and Hill (*14*); the effect of introducing T_2 relaxation is simply to restore the Lorentzian convolution term to Eq. [20], thus limiting the "sharpness" of any excitation to the natural linewidth $(1/\pi T_2)$. It is of interest to note that as a result, the limiting linewidth obtainable in a selective excitation experiment is governed by T_2 rather than by T_2^*, the decay constant due to static field inhomogeneity. This does not, however, lead of its own accord to any improvement in effective spectral resolution.

The analysis presented above deals only with the Bloch case of noninteracting classical magnetizations. While adequate for most purposes (e.g., weakly coupled spectra, proton-decoupled carbon-13 spectra), a variety of interesting experiments may

be envisaged involving strongly coupled systems, for which a more rigorous quantum mechanical approach would be necessary. Decoupling by a DANTE sequence and hole burning in strongly coupled systems fall into the latter category.

2.2. *The DANTE Pulse Sequence*

For a spin system close to equilibrium, Eq. [22] describes the transverse magnetization generated by an excitation $E(t)$, as a function of frequency. However, in many pulsed NMR experiments it is desirable to generate the maximum possible NMR signal, in which case the spin response is grossly nonlinear. In such cases the analysis presented in the preceding section is no longer valid, although it can often yield valuable qualitative results.

The DANTE pulse sequence is a case in point. Consider first the predictions of the linear approximation applied to a regular sequence of m pulses of radiofrequency field H_1 of duration Δt sec spaced at intervals of τ sec. This excitation can be represented in terms of some standard functions: an infinite train of δ functions $(\Delta t + \tau)$ sec apart [the "shah" function of Bracewell (*107*)] multiplied by a window function of width $m(\Delta t + \tau)$ sec (Bracewell's Π function) and convoluted with a window of width Δt sec (another Π function). The transforms of these standard functions are well known (another shah function and two sinc functions, respectively) and the convolution theorem can thus be used to deduce the transform of the pulse sequence.

In practice Δt is usually much less than τ, so that the last multiplication by the sinc function has very little effect in the frequency region of interest. This leads to a very simple form for the Fourier transform of the DANTE sequence: a series of δ functions $1/\tau$ Hz apart (the "sideband" frequencies mentioned earlier) convoluted with a complex sinc function, the real part of which is $1/m\tau$ Hz wide between zero-crossing points. Figure 3 illustrates how the convolution theorem leads to this result. Note that the transform of the overall window function has both a real and an imaginary part, since,

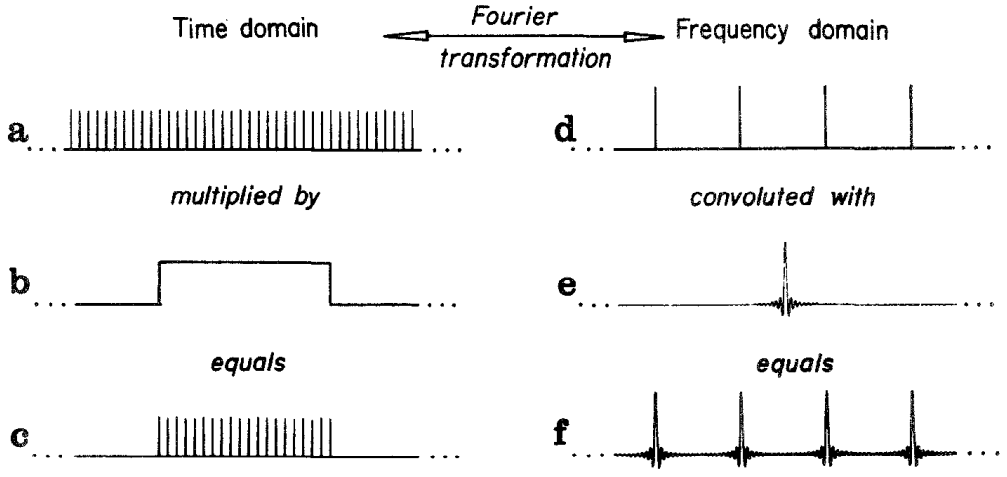

FIG. 3. A graphical illustration of the use of the convolution theorem to derive the transform of a DANTE sequence with $\Delta t \ll \tau$. Since the DANTE sequence is the product of (a) and (b), Fourier transformation of (c) produces (f), the convolution of (d) with (e). Only the real parts of the functions are shown.

as discussed in the previous section, zero time is taken to mean the end of the pulse sequence; only the real parts of the functions are shown in the diagram.

Consider a practical example consisting of ten pulses of flip angle 0.01 radians. If $\tau = 2$ msec, $\gamma H_1/2\pi = 1.59$ kHz and $\Delta t = 1$ μsec; then since $\Delta t \ll \tau$ it is possible to neglect the multiplication by the second sinc function. The spacing of the δ functions is 500 Hz, and these are convoluted by the first sinc function, which has a width of 50 Hz between the first zero crossings. If relaxation can be neglected, the excitation spectrum is given by

$$E(\Delta\omega) = i\gamma H_1[\text{shah}(1/\tau)\otimes\text{sinc}(1/m\tau)]. \quad [25]$$

For the above parameters the excitation maxima appear at offsets of 0, ± 500 Hz, ± 1000 Hz, etc., and have a magnitude $M_y/M_0 = 0.100$.

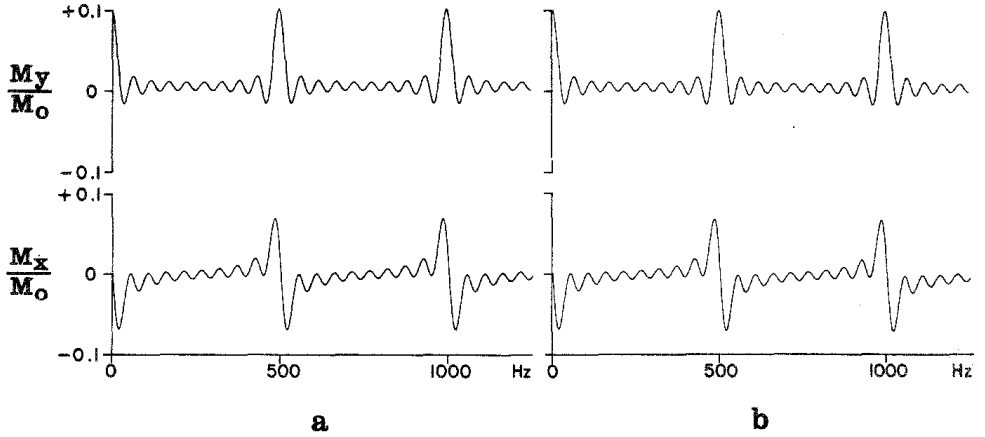

FIG. 4. Comparison between the excitation spectra predicted by (a) Fourier transformation of the pulse sequence according to the linear approximation, and (b) computer simulation based on the Bloch equations, for a ten-pulse DANTE sequence with overall flip angle $m\alpha = 0.1$ radians.

This may be compared with the results of the pictorial approach described in Section 1.2, which predicts a maximum Y magnetization of $M_0 \sin(0.1) = 0.998\ M_0$. It can be seen that there is good agreement between the predictions of the two approaches, since for this case the deviation from $M_z \simeq M_0$ is small and the linear approximation is justified. This is illustrated in Fig. 4, which shows excitation spectra obtained by computer simulation according to the Bloch equations, compared with the calculation based on Eq. [25]. Figure 5 shows the improvement in frequency selectivity obtained by increasing m to 50 for the same pulse interval as in Fig. 4 with a proportionately smaller flip angle.

The effects of nonlinearity are made clear in Fig. 6, which shows computer-simulated spectra for $m\alpha = \pi/2$ radians, equivalent to a selective 90° pulse on resonance, and normalized to $M_y/M_0 = 1$. The excitation spectrum predicted by the linear approximation differs mainly in the excitation maxima, which have $M_y/M_0 = \pi/2$ rather than the observed $M_y/M_0 = 1$. Figure 6 shows (a) the excitation spectrum predicted for $m = 20$ pulses according to the linear approximation, (b) the trigonometric sine of (a), and (c) the computer-simulated excitation spectrum. For the DANTE sequence under these conditions it can be seen that the actual excitation spectrum may usefully be approximated by the sine of the predicted linear response:

$$M_{xy}(\Delta\omega) = M_0 \sin[E(\Delta\omega)]. \quad [26]$$

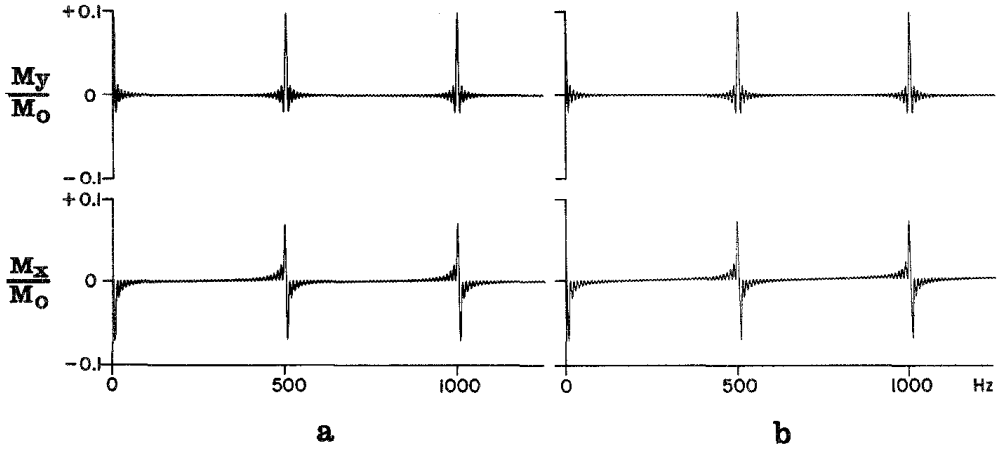

FIG. 5. A comparison similar to that of Fig. 4, but for a fifty-pulse sequence at the same repetition rate, showing the improvement in selectivity in the frequency domain. Note that the duration of the pulse sequence has increased by a factor of 5.

This approximation is particularly effective for the DANTE sequence because the degree of excitation is only large for a few evenly spaced frequencies.

The linear approximation permits two useful practical conclusions to be drawn about the DANTE sequence. First, as comparison between Figs. 4 and 5 shows, the ratio of the excitation at an exact sideband frequency to that approximately midway between sidebands increases with m, the number of pulses in the sequence. Second, the frequency selectivity increases in direct proportion to $m\tau$, the overall duration of the sequence. This can be measured as the width between zeros of the real sinc function, given by $1/(m\tau)$ Hz, or as the width at half-height, which is approximately $0.64/(m\tau)$ Hz. These values are slightly changed when the effects of nonlinearity are taken into account. For a

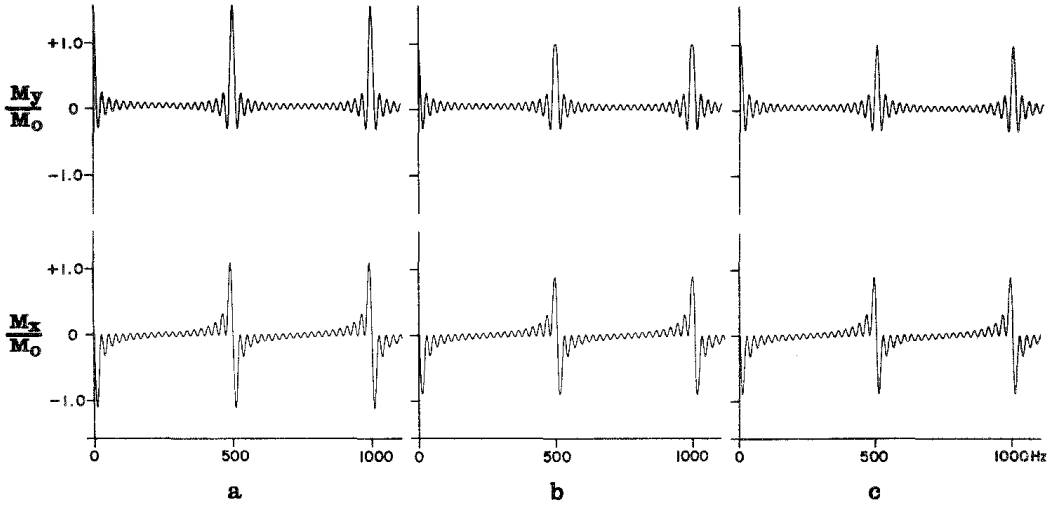

FIG. 6. An illustration of the effect of nonlinearity on excitation spectra for a twenty-pulse DANTE sequence of total flip angle $m\alpha = \pi/2$ radians. (a) The Fourier transform of the pulse sequence according to the linear approximation. (b) The trigonometric sine of (a). (c) The computer simulation based on the Bloch equations. Note that although the general features of (b) and (c) are similar, the main excitation peaks are broader in (b).

twenty-pulse DANTE sequence calculated to give a 90° pulse at exact resonance the width between zeros becomes about $0.92/(m\tau)$ Hz, and the width at half-height, $0.57/(m\tau)$ Hz.

However, since X magnetization appears in spectra as unwanted dispersion mode signals, a more useful guide to the selectivity of the pulse sequence is the absolute-value excitation spectrum $M_{xy}(\omega)$ (See Fig. 7a). For small total flip angles the excitation maxima have a width between zeros of approximately $2/(m\tau)$ Hz, and a half-height width of $1.21/(m\tau)$ Hz. Figure 7a compares the total transverse magnetization M_{xy} and its components M_x and M_y as a function of frequency for the case of a twenty-pulse DANTE sequence.

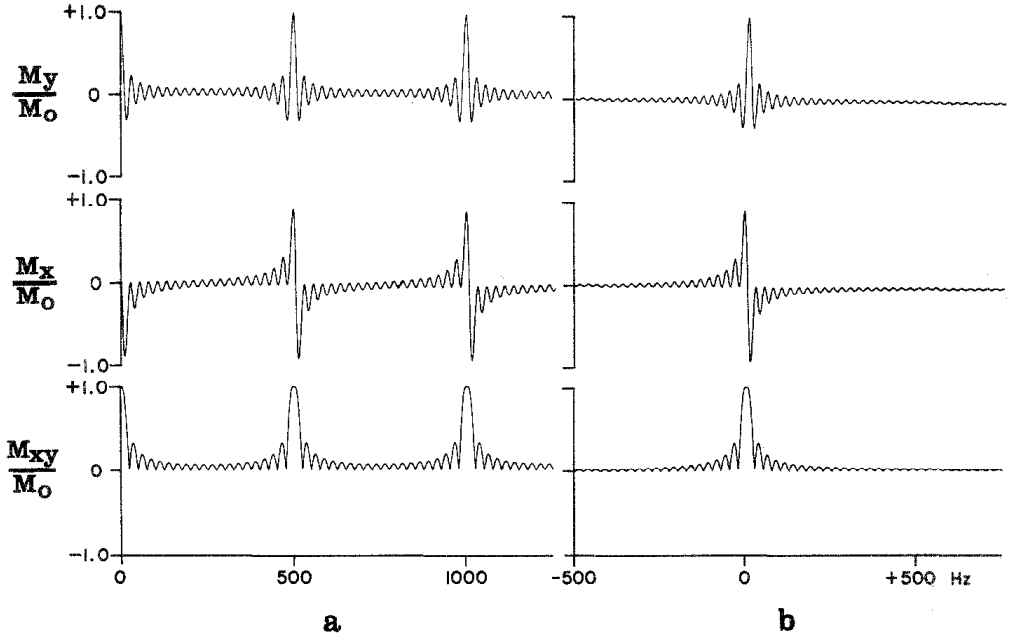

FIG. 7. (a) Excitation spectra for a twenty-pulse DANTE sequence, derived from the Bloch equations. For many purposes the selectivity is best judged from the absolute-value signal M_{xy}. (b) Excitation spectra corresponding to a single weak radiofrequency pulse of length 40 msec, equal to the total duration of the DANTE sequence used in (a), and of the same total flip angle $\pi/2$ radians.

It can be seen from Fig. 6 that away from the excitation maxima the linear approximation gives predictions close to the computer-simulated excitation spectra based on the macroscopic magnetization vector diagram. This is to be expected, since vectors far from the excitation maxima remain close to the Z axis throughout the DANTE sequence, and the linear approximation is justified.

Close to one of the sideband frequencies there is a better approximation than Eq. [26] available. Fourier analysis (rather than Fourier transformation) of the DANTE sequence shows a series of components spaced $1/\tau$ Hz apart in the frequency domain. For magnetization near one of these components, the effect of the DANTE sequence is similar to that of a low-level radiofrequency pulse of intensity $H_1\Delta t/(\Delta t + \tau)$. Figure 7 compares the computer-simulated excitation spectrum for a low-level radiofrequency pulse with that computed for a DANTE sequence with the same overall duration.

Thus for most practical purposes approximations are available which adequately describe the NMR response to a DANTE sequence. For some other purposes, for example, hole burning or solvent peak saturation, a steady-state analysis of the response to a regular sequence of pulses would be applicable (*103*, *105*). For certain applications the pictorial simulations based on the Bloch equations offer the most revealing description of the NMR behavior. A good example is the selective spin-locking experiment using a long DANTE sequence, for here the relaxation effects may be displayed very clearly.

2.3. The INFERNO experiment

Spin locking, or forced transitory precession (*70–76*), is one of the most effective methods of measuring transverse relaxation times in liquids, being considerably more tolerant of instrumental imperfections than spin-echo methods (*69*). The basic

TABLE 1

SEQUENCE OF EVENTS FOR THE INFERNO EXPERIMENT

(1)	Wait for equilibrium
(2)	Pulse of flip angle α about X axis
(3)	Delay τ
(4)	Repeat (2) and (3), m times
(5)	Pulse of flip angle β about Y axis
(6)	Delay τ
(7)	Repeat (5) and (6), n times
(8)	Acquire and transform free-induction decay

experiment consists in applying a 90° pulse to a magnetization, and then "locking" it in the transverse plane by applying a powerful radiofrequency field on resonance, phase shifted with respect to the 90° pulse, so as to align both magnetization and radiofrequency fields along the same axis in the rotating frame. The principal disadvantage of the experiment is that in order to spin lock all the lines in a spectrum it is necessary to employ a field strong compared to the width of the spectrum, leading to problems with transmitter design, sample overheating, or off-resonance effects.

These problems do not arise if resonances are studied individually, since then the only power requirement is that the radiofrequency field be strong compared to the linewidth (or multiplet width). This selective irradiation may be provided by a DANTE sequence, as in the INFERNO experiment (see Section 1.3). This uses two consecutive DANTE pulse sequences, both having the same pulse interval τ. The first, consisting of m pulses of flip angle α, where $m\alpha = \pi/2$, selectively rotates one magnetization down to lie along the Y axis in the rotating frame. The second sequence consists of n pulses of flip angle β, all shifted in radiofrequency phase by 90° with respect to the previous pulses, and provides a selective spin-locking field. In a typical experiment, m might be 50 and n several thousand. The sequence of events in an INFERNO experiment is summarized in Table 1.

As mentioned earlier the most fruitful theoretical approach to use here is to consider the longer DANTE locking sequence as being equivalent to a number of continuous low-level signals at the sideband frequences $\nu_0 + n/\tau$ Hz. Close to resonance, the effects

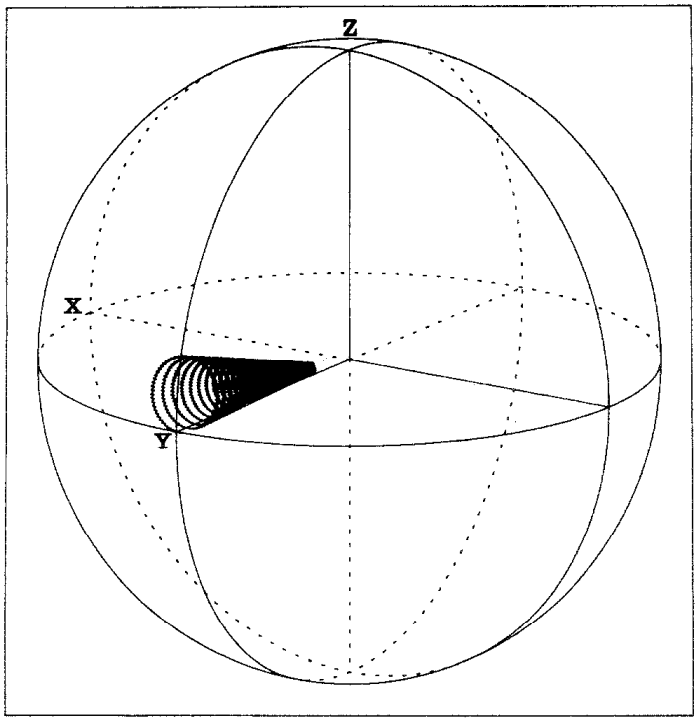

FIG. 8. The computer-simulated trajectory of a magnetization vector in a spin-locking experiment carried out by the INFERNO pulse sequence, viewed in a frame rotating at the "first sideband" frequency, ν_0 + 500 Hz. After the initial selective $\pi/2$ pulse, the spin-locking sequence used $\tau = 2$ msec and $\beta = \pi/30$ radians. The calculation is based on the Bloch equations with $T_1 = T_2 = 2$ sec, an offset of 499 Hz from ν_0, and a spin-locking time of 4 sec.

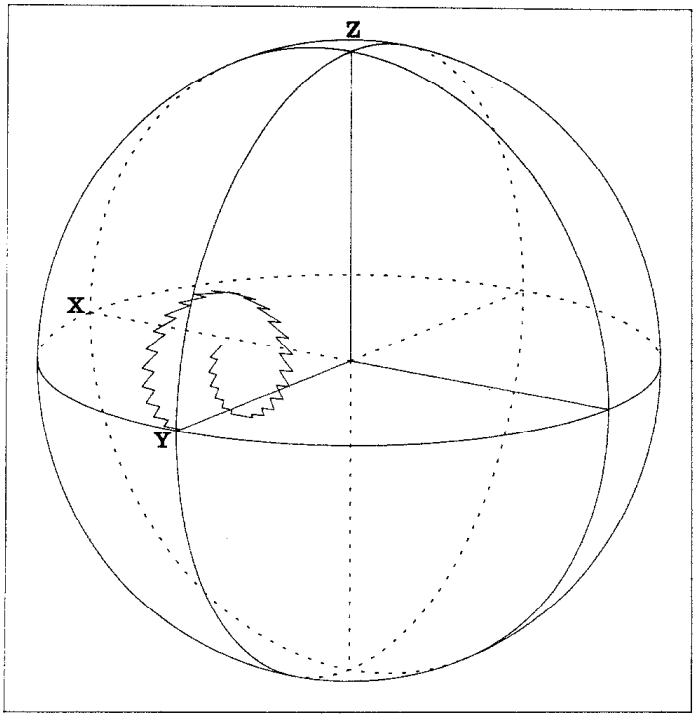

FIG. 9. A computer-simulated trajectory similar to Fig. 8, but with parameters changed in order to emphasize the zig-zig motion of the spin-locked magnetization, reflecting alternating periods of nutation and free precession. $T_1 = 10$ sec; $T_2 = 0.5$ sec; $\beta = \pi/12$ radians; $\tau = 10$ msec, and the offset is 99 Hz. The trajectory has been terminated after thirty pulses for the sake of clarity.

of one of these signals will predominate, and the experiment becomes equivalent to using a spin-locking field of intensity equal to the full transmitter power multiplied by the DANTE sequence duty cycle $\Delta t/(\Delta t + \tau)$. Thus by a suitable choice of β and τ any apparent spin-locking field strength may be obtained without changing the experimental hardware.

Figure 8 illustrates the trajectory of a magnetization close to resonance during an INFERNO experiment in a frame of reference rotating at the first sideband frequency, just as in Fig. 1. The effect of using a DANTE sequence rather than a low-level continuous field is to superimpose rapid small oscillations on the normal smoothly decaying spiral trajectory about the tilted effective field in the rotating frame. Figure 9 shows a similar experiment simulated using fewer pulses of larger flip angle in order to emphasize this zig-zag motion. The essence of the spin-locking experiment here is seen to lie in competition between rotation about the Y axis (nutation about the radiofrequency field) and about the Z axis (free precession due to the offset from resonance). It is this competition which prevents the dephasing of isochromats by forcing them to remain close to the Y axis in the rotating frame, counteracting the effects of static field inhomogeneity.

3. APPLICATIONS OF THE SELECTIVE PULSE SEQUENCE

3.1. Instrumental

All spectra were obtained on a Varian CFT-20 spectrometer operating at 20 MHz for carbon-13 and near 80 MHz for protons. The spectrometer had been slightly modified to improve the timing stability of the pulse generator but these changes are probably not essential for the applications described below. The selective pulse sequence requires small flip angles of the order of a few degrees each, and since the CFT-20 is designed to give a minimum pulse width of 1 μsec, it was found advantageous for most experiments to insert a resistive attenuator between the 20-MHz transmitter and the probe. This reduced the radiofrequency level such that a 90° pulse increased from 20 to 150 μsec. A more elegant solution (*77*) might be to generate pulses of small flip angle as a combination of two larger pulses 180° out of phase, so that the net nutation angle represents the difference in pulse widths. This would have the advantage of reducing problems of slow rise time and "phase glitch" effects (*93*).

A very simple software routine times a regular sequence of short pulses at a repetition rate determined by the offset of the chosen line from the transmitter frequency. In a case where the higher-order "sidebands" might accidentally irradiate other lines, it is sufficient to reset the transmitter frequency and readjust the repetition rate accordingly. The procedure is analogous to that used with field- or frequency-modulation sidebands in continuous-wave spectrometers. The selectivity of the irradiation in the frequency domain is determined by the overall duration of the pulse sequence. For example, a selectivity of the order of 1 Hz is achieved with a pulse sequence of duration 1 sec, the number of pulses in the sequence being determined by the repetition rate. In all other respects the spectrometer operates in the conventional manner, the free-induction signal following the new pulse sequence being acquired and transformed in the usual way.

Experiments that use both selective and nonselective pulses could be carried out by switching in the attenuator electronically when required, or by dispensing with it altogether. Irradiation of a broad band of frequencies essentially uniformly except for one chosen narrow band is achieved by means of a nonselective pulse and a selective sequence set 180° out of phase and adjusted to have the same overall flip angle.

Occasionally it is necessary to irradiate *two* arbitrarily chosen narrow regions within a spectrum. This requires the superposition of two independent selective pulse sequences in the time domain. Each sequence is timed to *end* at the same instant, but the sequences begin at different times and have different repetition rates. The control program examines the two superimposed sequences for near coincidences, substituting a single pulse of twice the width.

With these simple combinations many kinds of selective excitation experiment can be explored. Excitation patterns in the frequency domain that are more complicated than these are better implemented by the complete "synthesized excitation" method described by Tomlinson and Hill (*14*).

3.2. Proton-Coupled Carbon-13 Spectra from Individual Sites

The analysis of proton-coupled carbon-13 spectra can present considerable difficulty when spin multiplets from different carbon sites overlap. Since the coupling to directly bonded protons is often quite complicated, this situation is fairly common, and the task of unscrambling the fine structure may require careful manipulation of differential solvent shifts or temperature-dependence studies, as in a recent analysis of cyclopentadiene (*25*). By combining selective excitation and gated decoupling, it is possible to circumvent this problem, and display the multiplet structure from each carbon site as a separate "subspectrum," provided only that the fully decoupled carbon-13 resonances are sufficiently well resolved (*27–30*); a separation of the order of 1 Hz is adequate with normal linewidths.

The first stage of the experiment is to prepare the spin system with a nuclear Overhauser enhancement by noise irradiation of the protons. In the presence of the decoupler each carbon site will give rise to a single carbon-13 resonance line, and one of these is chosen for selective irradiation by a DANTE sequence, the others remaining as Z magnetization. The decoupling field is then removed, allowing the carbon-13 nuclei to precess according to the proton-coupled spin Hamiltonian, and the resulting free-induction signal is recorded. Fourier transformation yields a "subspectrum" containing the multiplet structure associated with only a single carbon site. Repetition of the process produces an array of different subspectra which together comprise the conventional proton-coupled spectrum. A penalty must be paid in sensitivity or instrument time since each subspectrum requires about the same accumulation time as the full coupled spectrum. However, it is seldom necessary to record the entire array of subspectra, and it is often possible to excite suitable subspectra in pairs which have no overlapping lines. An important bonus associated with this method is the significantly improved digital resolution in the frequency domain, a feature that is particularly useful for the study of fine structure (*30*). It arises because a subspectrum requires a much narrower spectral width than the full coupled spectrum, so that the data points may be more finely disposed without folding unwanted lines into the spectrum.

Figure 10 shows an example of the application of this method to the spectrum of menthone. The top trace shows the decoupled carbon-13 spectrum with lines (A) through (I) from the nine different carbon sites. The corresponding subspectra are shown in traces (a) through (i); in each case the selectivity sufficed to remove all interference from other spin multiplets, the solvent, and the lock material. The lowest trace shows the conventional proton-coupled carbon-13 spectrum, and illustrates the

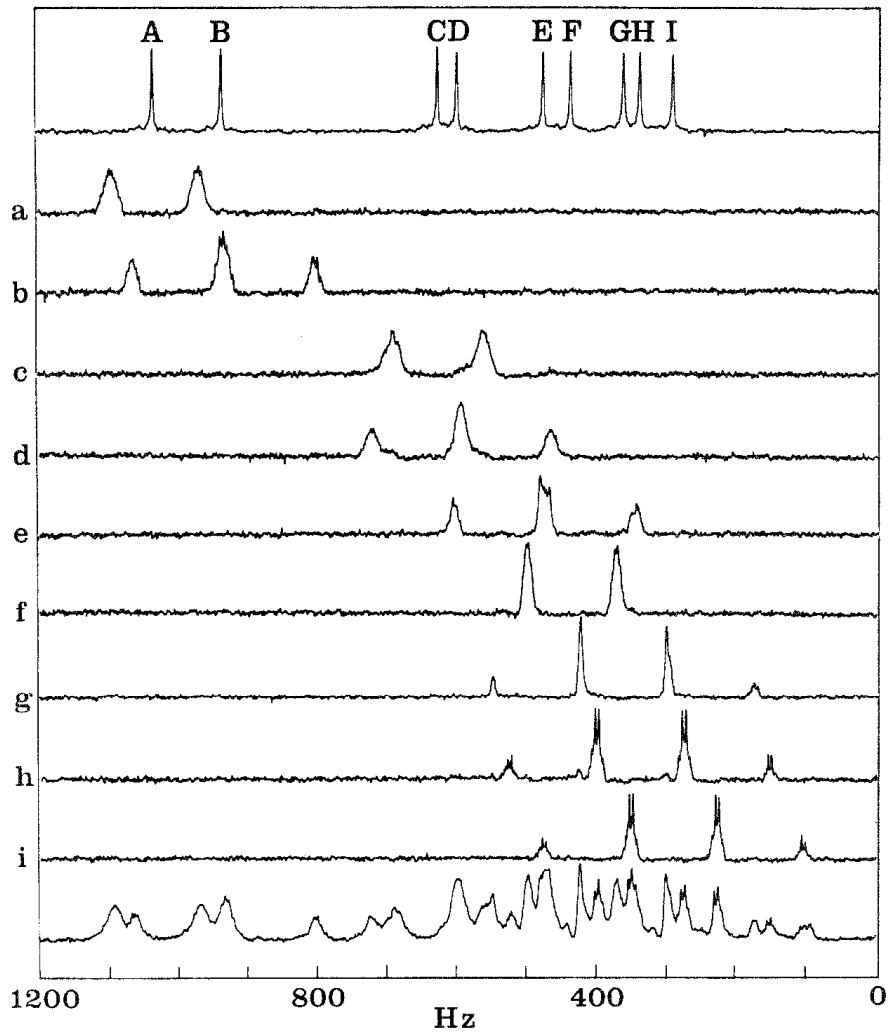

FIG. 10. The conventional proton-decoupled carbon-13 spectrum of menthone (top trace) showing resonances from nine chemically distinct sites. Traces (a) through (i) show proton-coupled subspectra from sites (A) through (I), obtained by selective excitation by a DANTE sequence and gated decoupling. The lowest trace shows the conventional proton-coupled spectrum illustrating the complicated overlap of spin multiplets.

complex overlap problem. Subspectra (h) and (i) have been used to provide evidence about the rotameric equilibrium in menthone (*29*). It will be noticed that some of the spin multiplets show a significant asymmetry about the chemical shift frequency, a consequence of strong coupling in the proton spectrum (*109*).

3.3 Suppression of Unwanted Signals

The investigation of biochemical systems in aqueous solution has been severely hampered by the limitations imposed on the dynamic range when the signal is converted into digital form in a Fourier transform spectrometer, and even with heavy water as solvent, the residual HDO peak can be troublesome. Several ingenious experiments have been suggested to suppress unwanted strong solvent peaks. The selective pulse

sequence may be employed in a variety of ways to alleviate such problems. A long regular sequence of pulses may be used to saturate a particular resonance selectively, the rest of the spectrum being examined by a subsequent nonselective pulse. Formally this experiment would be described by the steady-state solution for the response to a regular sequence of pulses (*103*, *105*) provided that the sequence is sufficiently long, rather than the transient solutions presented in Section 2.2. The result is very similar to the application of a continuous weak radiofrequency field. Figure 11 illustrates the application to the proton spectrum of the *cis*-3,5 dimethylpiperidinium ion, showing saturation of the water line by a selective pulse sequence several seconds long. If the duration of the "saturation" sequence is comparable with or shorter than the relevant relaxation times, it is still possible to achieve almost complete elimination of the irradiated line. Although the net nuclear magnetization from the sample may be

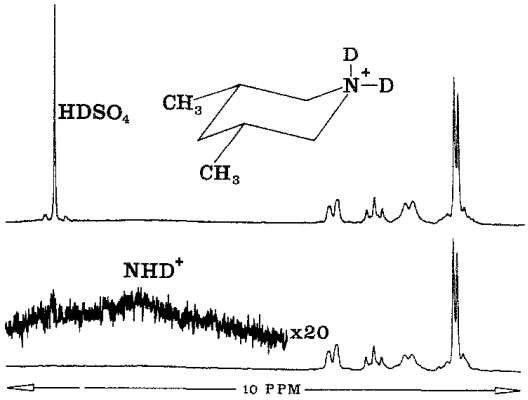

FIG. 11. Proton spectra of the *cis*-3,5 dimethylpiperidinium ion in D_2SO_4 solution, with and without saturation of the solvent proton line by a DANTE sequence of several seconds' duration prior to the usual $\pi/2$ excitation pulse. A weak broad line from NHD^+ is detectable in the trace at increased gain, normally masked by the tail of the strong solvent line.

negligible, local magnetization components are merely dispersed by transient nutations in an inhomogeneous effective field, mainly because the radiofrequency field is spatially inhomogeneous (*5*, *46*, *47*, *110*).

Selective excitation (rather than saturation) may also be used to remove unwanted lines. For example, a selective 90° pulse followed by a nonselective 90° pulse leaves the chosen line with negligible transverse magnetization, but the rest of the spectrum with full transverse components. A rather better variation inverts the radiofrequency phase between the selective and nonselective pulses, which may have arbitrary but equal flip angles. Selective 180° pulses are also useful. Patt and Sykes (*7*) have described a method of eliminating solvent peaks, particularly HDO in biochemical solutions, by inverting all resonances with a nonselective 180° pulse, and then exciting the spectrum at the precise instant that the HDO peak passes through the null condition. The method relies on the faster spin–lattice relaxation of the large solute molecules, but suffers intensity distortions due to different relaxation rates. Substitution of a *selective* 180° pulse would largely circumvent this intensity problem, and improve the sensitivity of the method. This experiment, using a low-level pulse rather than a DANTE sequence, has recently been described by Gupta (*11*).

3.4. *"Hole Burning"*

If a resonance line is inhomogeneously broadened, it is possible in principle to saturate a narrow region of the line but leave the remainder essentially unaffected. The effect of the strong irradiation is essentially confined to a small restricted volume somewhere within the sample, other regions being off-resonance. Bloembergen *et al.* (*90*) describe this phenomenon as burning a hole in the line. The experiment has remained something of a curiosity, but has been employed in double resonance (*91*) and in studies of linewidths in rubber (*92*). The technique requires an extremely stable and finely tunable radiofrequency oscillator, or a suitable sideband of the master oscillator.

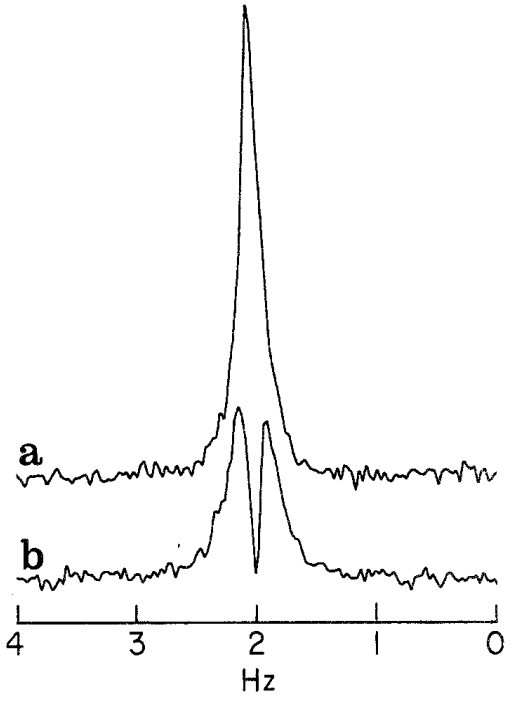

FIG. 12. One of the inner lines of the proton-coupled carbon-13 quartet of methyl iodide, (a) before and (b) after application of a hole-burning DANTE sequence lasting approximately 7 sec. The linewidth is 0.3 Hz, a typical value for the CFT-20, and the width of the hole approximately 0.1 Hz.

In a Fourier transform spectrometer an attractive alternative is a long selective pulse sequence with low duty cycle.

Figure 12 shows a hole burnt in one component of the proton-coupled carbon-13 quartet of methyl iodide by this method. A DANTE sequence of 350 pulses of flip angle $\pi/300$ radians, lasting about 7 sec, was used to burn the hole, followed by an observation pulse of flip angle $\pi/6$ radians. This resulted in a hole approximately 0.1 Hz wide, or about one-third of the limiting instrument linewidth. Because the pulse sequence used lasted rather less than T_1, the hole represents, not the steady-state saturation reported previously (*90–92*), but a highly selective transient excitation of restricted regions of the sample.

Since a hole may never be narrower than the natural linewidth, the method may be used to give a rough indication of differences in natural linewidth for assignment purposes, as well as to provide a simple test for inhomogeneous broadening.

3.5. *Selective Spin Locking*

The INFERNO experiment described in Section 2.2 may be used to measure spin–lattice relaxation times in the rotating frame $T_{1\varrho}$, for individual lines in a spectrum. In liquids, these relaxation times carry similar information to T_2, and hence have considerable interest. The experiment consists in measuring the magnetization remaining after increasing periods of spin locking, normally produced by incrementing the number n of locking pulses. Two approaches recommend themselves: acquire and transform a series of free-induction decays after increasing periods of spin locking, after the manner of a conventional inversion–recovery experiment; or sample the magnetization during the interpulse delays, giving a signal decaying with time constant $T_{1\varrho}$. The latter "transparent" method is more difficult, but is a very efficient experiment as it records an entire $T_{1\varrho}$ decay at once. Figure 13 shows the results of spin-locking experiments on the proton-decoupled carbon-13 resonances of pyridine, using the

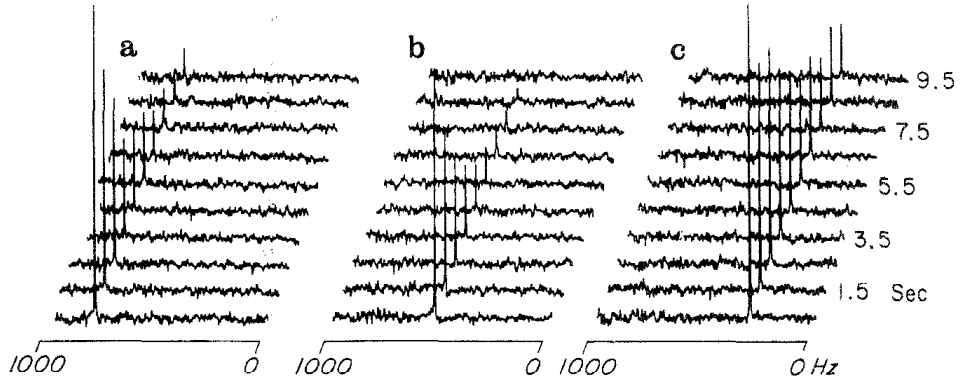

FIG. 13. The decay of transverse magnetization in selective spin-locking experiments on the three proton-decoupled carbon-13 resonances of pyridine, (a) C2, (b) C4, and (c) C3. The same spectral window was used in each case; in a conventional spectrum the three lines appear at offsets of 789, 531, and 301 Hz, respectively. The INFERNO pulse sequence was used with an effective spin-locking field intensity of about 20 Hz.

former of the two methods in order to emphasize the selective nature of the experiment. Because the spin-locking method is less affected by instrumental shortcomings such as radiofrequency field inhomogeneity and pulse irreproducibility, these decays are rather longer than those obtained by conventional spin-echo refocusing experiments on this instrument, although at the present level of experimental technique the results are still sensitive to instrumental shortcomings.

3.6. *The Study of Chemical Exchange by Saturation Transfer*

Forsén and Hoffman (*41–43*) described a powerful double-resonance experiment for monitoring chemical exchange processes which take place on a time scale comparable with relaxation. In this technique the longitudinal magnetization of a resonance is measured as a function of time after the perturbation of another resonance with which it is exchanging. This perturbation may be the imposition of a saturating field, or a 180° pulse, or various other possibilities.

The experiment has been performed using low-level pulses (*111*) and saturating fields (*112–116*) in Fourier transform NMR. The largest effects are seen when the

longitudinal magnetizations of the exchanging sites are monitored after one resonance is selectively inverted. This selective inversion may easily be achieved using a DANTE sequence with cumulative flip angle 180° on resonance. The expressions for magnetization at sites A and B as a function of the delay τ_x between inversion and sampling are

$$M_z^A/M_0^A = 1 - (2k_A/\beta)\{\exp[-\tfrac{1}{2}(\alpha-\beta)\tau_x] - exp[-\tfrac{1}{2}(\alpha+\beta)\tau_x]\}, \quad [27]$$

$$M_z^B/M_0^B = 1 - (1/\beta)\{(\beta + R_B - R_A)\exp[-\tfrac{1}{2}(\alpha+\beta)\tau_x] + (\beta + R_A - R_B)\exp[-\tfrac{1}{2}(\alpha-\beta)\tau_x]\}, \quad [28]$$

where

$$\alpha = R_A + R_B, \qquad \beta = [(R_A - R_B)^2 + 4k_A k_B]^{1/2},$$

and

$$R_A = k_A + (1/T_{1A}), \qquad R_B = k_B + (1/T_{1B}).$$

TABLE 2

SEQUENCE OF EVENTS FOR OBTAINING A DIFFERENCE SPECTRUM AFTER SELECTIVE INVERSION

(1)	Wait for equilibrium
(2)	Nonselective 90° sampling pulse
(3)	Acquire free induction decay and add to store
(4)	Wait for equilibrium
(5)	DANTE pulse sequence with 180° flip angle on resonance
(6)	Exchange delay τ_x
(7)	Nonselective 90° sampling pulse
(8)	Acquire free-induction decay and subtract from store
(9)	Improve signal-to-noise by repeating (1) through (8)
(10)	Fourier transform averaged signal to obtain difference spectrum

Thus by monitoring the recovery curves of sites A and B it is possible in favourable cases to extract both the exchange rate constants, k_A and k_B, and the longitudinal relaxation times, T_{1A} and T_{1B}, of the two sites.

In order to obtain cleaner spectra and more reproducible results, a form of difference spectroscopy may be used (*111*, *117*). Time averaging is carried out by alternately co-adding the transients following an isolated 90° pulse and subtracting those obtained after selective inversion. This difference signal transforms to a spectrum which is the difference between the equilibrium spectrum and the perturbed spectrum. The overall sequence of events is summarized in Table 2. The method thus yields spectra showing the deviation from equilibrium longitudinal magnetization caused by the selective inversion, allowing the transfer of magnetization to be followed as a function of time, without interference from any overlapping lines.

Figure 14 shows a series of such difference spectroscopy experiments with increasing exchange delays τ_x, performed on the 3,5 carbon resonances of the 1,2,6-trimethyl-piperidinium ion in slightly alkaline solution. This undergoes slow interconversion between the equatorial *N*-methyl and axial *N*-methyl stereoisomers, so that the inversion

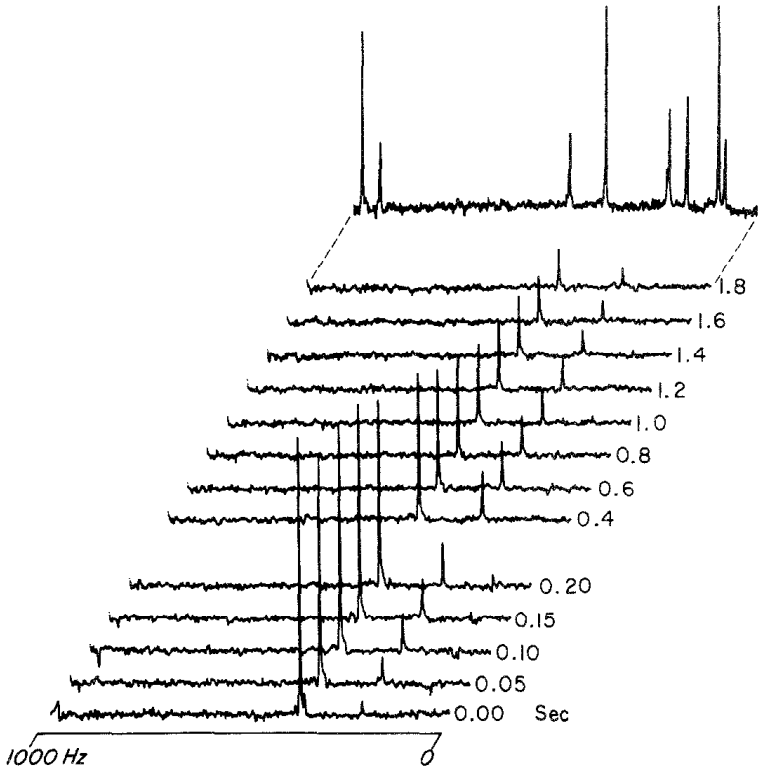

FIG. 14. Study of chemical exchange rates by a selective population inversion experiment, using a DANTE pulse sequence of seventeen pulses of flip angle $\pi/17$ radians, lasting 45 msec. The top trace shows the full proton-decoupled carbon-13 spectrum of the 1,2,6-trimethylpiperidinium ion, containing lines from both the interconverting equatorial and axial *N*-methyl stereoisomers. The difference spectra below were obtained by subtracting the inverted and conventional free-induction decays, leading to spectra showing the decrease in Z magnetization caused by the selective inversion. The time axis represents the delay τ_x after selective inversion of the low-field (equatorial *N*-methyl stereoisomer) line, showing the transfer of negative Z magnetization to the weaker high-field line of the axial stereoisomer.

of the 3,5 carbon resonance of the equatorial species (the left-hand line of Fig. 14) causes transfer of negative Z magnetization to the 3,5 resonances of the axial stereoisomer. The difference spectra thus show a biexponential decay for the equatorial resonance recovering from inversion, while the axial resonance first loses magnetization to the equatorial resonance and then returns slowly to equilibrium. The time scale of Fig. 14 is split in order to show the growth of magnetization exchange, followed by the slower, relaxation-limited return to equilibrium. The conventional spectrum in the diagram illustrates an important advantage of the difference spectroscopy technique—the 3,5 resonance of the axial stereoisomer overlaps with the axial *N*-methyl line, making it difficult to measure accurately the intensity changes of the former. An analysis of the results yields the values $T_{1A} = T_{1B} = 1.1 \pm 0.2$ sec, $k_A = 3.4 \pm 0.5$ sec^{-1}, and $k_B = 1.6 \pm 0.5$ sec^{-1}.

4. DISCUSSION

In the preceding pages some general principles for selective excitation in Fourier transform NMR have been established, and applied to one particular family of

experiments based on the DANTE plus sequence. A range of techniques involving transient and steady-state selective irradiation has been shown to be possible on simple conventional instrumentation.

The use of the linear approximation and Fourier transformation methods greatly facilitates the design of selective experiments, by providing an easy link between a desired excitation spectrum and the necessary pulse sequence. The biggest advantage of the DANTE sequence is of course its simplicity; on the CFT-20 the added pulse programming can amount to less than two dozen locations. In the vast majority of cases the characteristic multiple sinc function excitation spectra are quite adequate; however, in more critical situations the use of Fourier transform concepts can allow the selectivity of the DANTE sequence to be enhanced without recourse to the full Tomlinson/Hill synthesized excitation experiment (*14*).

When it is desirable to excite a particularly narrow spectral region, the lobes of the sinc functions in the excitation spectrum can cause problems by giving limited excitation to neighboring resonances. The ideal rectangular "window" function spectrum can be more closely approached by modulating the DANTE sequence with a sinc function envelope (or possibly just a crude approximation to it). Thus by giving each pulse in a DANTE sequence an amplitude (or more simply a width) determined by a preset recipe such that the flip angles of successive pulses follow an approximate $\sin(t)/t$ dependence, a more rectangular window excitation spectrum may be produced.

In wide and crowded spectra the presence of more than one maximum in the excitation spectrum (i.e., the presence of many sidebands) may be a problem. The number of these sidebands may be reduced by phase modulating the pulses in a DANTE sequence. For example, alternating the phases of successive pulses to give alternate positive and negative flip angles leads to an excitation spectrum with maxima not at $\nu_0 + n/\tau$ as in a conventional DANTE experiment, but at $\nu_0 + 1/(2\tau) + n/\tau$. This means in effect that to excite the same frequency a phase-alternated DANTE sequence would use twice the pulse repetition rate of a normal sequence, giving twice the sideband spacing.

The linearity of the Fourier transform operation (the transform of the sum of two functions is the sum of their individual transforms) means that more complex excitation spectra may be produced by adding together different pulse sequences. Thus the construction of a pulse sequence by adding two DANTE sequences with pulse spacing τ_1 and τ_2 leads to an excitation spectrum containing maxima at $\nu_0 + n/\tau_1$ and $\nu_0 + n/\tau_2$. This allows the simultaneous excitation of two independent frequencies, as illustrated in Fig. 15; phase coherence between the two excited resonances is achieved by finishing both DANTE sequences at the same moment.

The combination of excitation by DANTE sequence and gated decoupling, a possibility first envisaged by Müller *et al.* (*118*), is an example of a useful class of experiments having no counterparts in continuous-wave or slow-passage spectroscopy. The time-domain character of Fourier transform spectroscopy makes it possible to change experimental conditions between excitation and observation, allowing correlations to be made between different types of spectrum of the same sample. Thus in the example given in Fig. 10, by exciting a decoupled carbon-13 resonance and measuring the response under proton-coupled conditions it is possible to obtain the multiplet structure associated with one decoupled line. The experiment could equally,

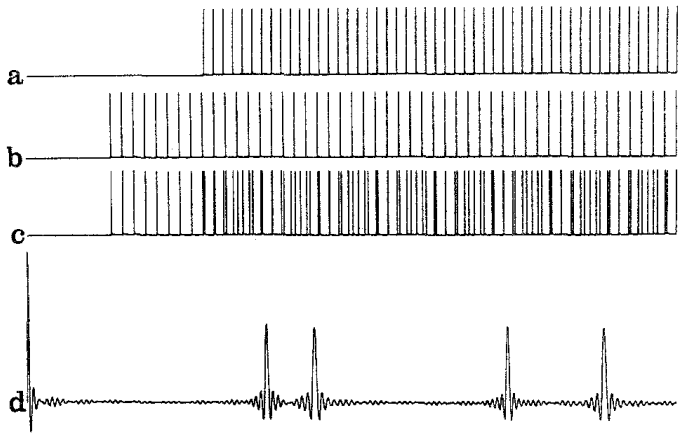

FIG. 15. The superposition (c) of two DANTE pulse sequences (a) and (b) with different repetition rates. Trace (d) shows the frequency-domain excitation spectrum calculated by Fourier transformation of the time-domain pattern (c). This scheme permits selective irradiation of two arbitrary frequencies.

although less usefully, have been performed by exciting one line in the coupled spectrum and acquiring the free-induction decay with proton decoupling. In this way the chemical shift corresponding to any line in the coupled spectrum may be measured.

Naturally the technique is not restricted to carbon-13–proton double resonance; similar experiments could be envisaged for any pair of coupled nuclei, or for homonuclear coupling between widely separated groups of resonances. The analysis of spectra containing two types of heteronuclear coupling, for example, partially fluorinated compounds, could be greatly facilitated by observing coupled carbon-13 subspectra after selective excitation in the presence of proton or fluorine decoupling. In very complex carbon-13 spectra, off-resonance decoupling is frequently used to obtain information about multiplicity. Selective excitation could remove overlap in the off-resonance decoupled spectrum by changing the decoupling conditions from noisy on-resonance to coherent off-resonance.

A more prosaic advantage of being able to examine small regions of coupled spectra at a time is that the available digitization may be more effectively used without interference from folded lines. This has been exploited in some high-resolution measurements on the proton-coupled carbon-13 spectrum of pyridine (*30*).

Several more-complex methods have recently been proposed for decomposing coupled carbon-13 spectra into multiplets from different carbon sites (*118–122*), using the technique of double Fourier transform NMR (*123–125*). For small systems the selective excitation method has the advantages of simplicity and better signal-to-noise ratio, although the latter no longer applies in more complex spectra, since the double Fourier transform techniques acquire information about all carbon sites in a molecule in a single experiment. Some two-dimensional spectroscopy techniques (those based on "*J*" or "spin-echo" spectroscopy) have the added advantage of providing linewidths which in principle are limited not by magnetic field inhomogeneity but by T_2 relaxation. The "proton flip" two-dimensional *J*-spectroscopy experiment can also provide extra information about strong coupling (*122*).

The study of chemical exchange by monitoring the transfer of saturation was first performed in continuous-wave mode by Forsén and Hoffman (*41–43*), but lends itself

readily to Fourier transform experiments (*111–116*). Of the many techniques possible, one of the most powerful is to invert a magnetization at site A, and monitor the recovery both of this resonance and that of site B with which it is exchanging. Together with difference spectroscopy, as described in Section 3.6, the use of the DANTE sequence for selective inversion here allows a simple and clean determination of exchange rate constants. The full range of rate constants between those accessible by line shape analysis and those comparable with relaxation rates may be covered. Three site exchange problems (*43*) may be dealt with using single and dual DANTE sequences for inversion.

The measurement of T_2 (or the similar parameter $T_{1\varrho}$) in high-resolution NMR by Fourier transform methods has proved a difficult goal to achieve on a routine basis. One possible response to the problem is to use instrumentally less demanding techniques on individual resonances, rather than try to measure all resonances in a spectrum simultaneously. The INFERNO experiment is simple and effective, and in its "transparent" version, is capable of obtaining results more quickly than nonselective methods when applied to small molecules. Dual or multiple DANTE sequences would enhance the speed of the method by allowing more than one resonance to be spin locked at once.

The hole-burning experiment is a quick and useful test for inhomogeneous broadening. A number of other possible uses exist; for instance it should be feasible to identify regressively connected transitions in coupled systems by burning a hole in one line and seeing which other lines are affected. In more general terms, the selective perturbation of populations in strongly coupled systems can lead to a variety of useful and interesting effects.

All the experiments described in this paper may of course be performed using low-level continuous radiofrequency pulses, rather than DANTE sequences, on spectrometers with weak pulse facilities. The DANTE sequence does, however, have the advantage that total flip angle and selectivity may be controlled independently, without changing the pulse power. The wide range of selective experiments possible has yet to be fully exploited; the DANTE family of techniques represents one approach to performing such experiments on conventional Fourier transform spectrometers. A simple selective excitation program using the DANTE sequence, SELEX MK6, has been written for unmodified CFT-20 spectrometers, and is available from the authors on request.

ACKNOWLEDGMENTS

This work was made possible by an equipment grant and a research studentship from the Science Research Council. The authors gratefully acknowledge several helpful discussions with Dr. H. D. W. Hill and with Dr. M. J. T. Robinson, who also provided the sample of 1,2,6-trimethylpiperidinium chloride.

REFERENCES

1. J. SCHAEFER, *J. Magn. Resonance* **6**, 670 (1972).
2. J. P. JESSON, P. MEAKIN, AND G. KNEISSEL, *J. Amer. Chem. Soc.* **95**, 618 (1973).
3. I. D. CAMPBELL, C. M. DOBSON, G. JEMINET, AND R. J. P. WILLIAMS, *FEBS Lett.* **49**, 115 (1974).
4. H. E. BLEICH AND J. A. GLASEL, *J. Magn. Resonance* **18**, 401 (1975).
5. D. I. HOULT, *J. Magn. Resonance* **21**, 337 (1976).
6. N. R. KRISHNA, *J. Magn. Resonance* **22**, 555 (1976).

7. S. L. PATT AND B. D. SYKES, *J. Chem. Phys.* **56,** 3182 (1972).
8. F. W. BENZ, J. FEENEY, AND G. C. K. ROBERTS, *J. Magn. Resonance* **8,** 114 (1972).
9. E. S. MOOBERRY AND T. R. KRUGH, *J. Magn. Resonance* **17,** 128 (1975).
10. T. R. KRUGH AND W. C. SCHAEFER, *J. Magn. Resonance* **19,** 99 (1975).
11. R. K. GUPTA, *J. Magn. Resonance* **24,** 461 (1976).
12. S. ALEXANDER, *Rev. Sci. Instrum.* **32,** 1066 (1961).
13. A. G. REDFIELD AND R. K. GUPTA, *J. Chem. Phys.* **54,** 1418 (1971).
14. B. L. TOMLINSON AND H. D. W. HILL, *J. Chem. Phys.* **59,** 1775 (1973).
15. A. G. REDFIELD, S. D. KUNZ, AND E. K. RALPH, *J. Magn. Resonance* **19,** 114 (1975).
16. J. DADOK AND R. F. SPRECHER, *J. Magn. Resonance* **13,** 243 (1974).
17. R. K. GUPTA, J. A. FERRETTI, AND E. D. BECKER, *J. Magn. Resonance* **13,** 275 (1974).
18. Y. ARATA AND H. OZAWA, *J. Magn. Resonance* **21,** 67 (1976).
19. J. A. FERRETTI AND R. R. ERNST, *J. Chem. Phys.* **65,** 4283 (1976).
20. F. W. WEHRLI AND T. WIRTHLIN, "Interpretation of Carbon-13 NMR Spectra," Heyden, London, 1976, and references therein.
21. M. HANSEN AND H. J. JAKOBSEN, *J. Magn. Resonance* **20,** 520 (1975).
22. L. ERNST, D. N. LINCOLN, AND V. WRAY, *J. Magn. Resonance* **21,** 115 (1976).
23. V. A. CHERTKOV AND N. M. SERGEYEV, *J. Magn. Resonance* **21,** 159 (1976).
24. L. ERNST, E. LUSTIG, AND V. WRAY, *J. Magn. Resonance* **22,** 459 (1976).
25. V. A. CHERTKOV, Y. K. GRISHIN, AND N. M. SERGEYEV, *J. Magn. Resonance* **24,** 275 (1976).
26. L. ERNST, V. WRAY, V. A. CHERTKOV, AND N. M. SERGEYEV, *J. Magn. Resonance* **25,** 123 (1977).
27. R. FREEMAN, Sixth Conference on Molecular Spectroscopy, Durham, England, March 1976; published as Chap. 2 of "Molecular Spectroscopy" (A. R. West, Ed.), Heyden, London, 1977.
28. G. BODENHAUSEN, R. FREEMAN, AND G. A. MORRIS, *J. Magn. Resonance* **23,** 171 (1976).
29. R. FREEMAN, G. A. MORRIS, AND M. J. T. ROBINSON, *J. Chem. Soc. Chem. Commun.,* 754 (1976).
30. R. FREEMAN, G. A. MORRIS, AND D. L. TURNER, *J. Magn. Resonance* **26,** 373 (1977).
31. K. G. R. PACHLER AND P. L. WESSELS, *J. Magn. Resonance* **12,** 337 (1973).
32. S. SØRENSEN, R. S. HANSEN, AND H. J. JAKOBSEN, *J. Magn. Resonance* **14,** 243 (1974).
33. H. J. JAKOBSEN, S. A. LINDE, AND S. SØRENSEN, *J. Magn. Resonance* **15,** 385 (1974).
34. A. A. CHALMERS, K. G. R. PACHLER, AND P. L. WESSELS, *J. Magn. Resonance* **15,** 415 (1974).
35. A. A. CHALMERS, K. G. R. PACHLER, AND P. L. WESSELS, *Org. Magn. Resonance* **6,** 445 (1974).
36. S. A. LINDE AND H. J. JAKOBSEN, *J. Amer. Chem. Soc.* **98,** 1041 (1976).
37. N.J. KOOLE, D. KNOL, AND M. J. A. DEBIE, *J. Magn. Resonance* **21,** 499 (1976).
38. N. J. KOOLE AND M. J. A. DEBIE, *J. Magn. Resonance* **23,** 9 (1976).
39. H. J. JAKOBSEN AND H. BILDSØE, *J. Magn. Resonance* **26,** 183 (1977).
40. R. A. HOFFMAN AND S. FORSÉN, "Progress in Nuclear Magnetic Resonance Spectroscopy" (J. W. Emsley, J. Feeney, and L. H. Sutcliffe, Eds.), Vol. 1, p. 15, Pergamon, Oxford, 1966.
41. S. FORSÉN AND R. A. HOFFMAN, *J. Chem. Phys.* **39,** 2892 (1963).
42. S. FORSÉN AND R. A. HOFFMAN, *Acta Chem. Scand.* **17,** 1787 (1963).
43. S. FORSÉN AND R. A. HOFFMAN, *J. Chem. Phys.* **40,** 1189 (1964).
44. R. A. HOFFMAN AND S. FORSÉN, *J. Chem. Phys.* **45,** 2049 (1966).
45. R. FREEMAN AND S. WITTEKOEK, *in* "Proceedings of the 15th Colloque AMPERE Grenoble (1968)," p. 205, North–Holland, Amsterdam, 1968.
46. R. FREEMAN AND S. WITTEKOEK, *J. Magn. Resonance* **1,** 238 (1969).
47. E. J. WELLS AND K. H. ABRAMSON, *J. Magn. Resonance* **1,** 378 (1969).
48. R. FREEMAN, S. WITTEKOEK, AND R. R. ERNST, *J. Chem. Phys.* **52,** 1529 (1970).
49. A. R. MUIR AND D. W. TURNER, *J. Chem. Soc. Chem. Commun.,* 286 (1971).
50. M. F. AUGUSTEIJN, W. M. M. J. BOVÉE, S. EMID, A. F. MEHLKOPF, AND J. SMIDT, *J. Magn. Resonance* **7,** 301 (1972).
51. C. W. M. GRANT, L. D. HALL, AND C. M. PRESTON, *J. Amer. Chem. Soc.* **95,** 7742 (1973).
52. A. BRIGUET, J.-L. CULTY, J.-C. DUPLAN, AND J. DELMAU, *J. Phys. E.* **7,** 791 (1974).
53. R. FREEMAN, H. D. W. HILL, B. L. TOMLINSON, AND L. D. HALL, *J. Chem. Phys.* **61,** 4466 (1974).
54. C. L. MAYNE, D. W. ALDERMAN, AND D. M. GRANT, *J. Chem. Phys.* **63,** 2514 (1975).
55. L. D. HALL and H. D. W. HILL, *J. Amer. Chem. Soc.* **98,** 1269 (1976).
56. C. L. MAYNE, D. M. GRANT, AND D. W. ALDERMAN, *J. Chem. Phys.* **65,** 1684 (1976).

57. D. W. ALDERMAN, J. J. LED, J. PEDERSEN, AND N. F. ANDERSEN, *J. Magn. Resonance* **21,** 77 (1976).
58. C. LAPRAY, A. BRIGUET, J.-C. DUPLAN, AND J. DELMAU, *J. Magn. Resonance* **23,** 129 (1976).
59. W. M. M. J. BOVÉE, *J. Magn. Resonance* **24,** 327 (1976).
60. I. SOLOMON, *Phys. Rev.* **99,** 559 (1955).
61. I. SOLOMON AND N. BLOEMBERGEN, *J. Chem. Phys.* **25,** 261 (1956).
62. I. D. CAMPBELL AND R. FREEMAN, *J. Chem. Phys.* **58,** 2666 (1973).
63. I. D. CAMPBELL AND R. FREEMAN, *J. Magn. Resonance* **11,** 143 (1973).
64. D. CANET, *J. Magn. Resonance* **23,** 361 (1976).
65. R. K. HARRIS AND R. H. NEWMAN, *J. Magn. Resonance* **24,** 449 (1976).
66. E. L. HAHN AND D. E. MAXWELL, *Phys. Rev.* **84,** 1246 (1951).
67. E. L. HAHN AND D. E. MAXWELL, *Phys. Rev.* **88,** 1070 (1952).
68. J. G. POWLES AND A. HARTLAND, *Proc. Phys. Soc.* **77,** 273 (1961).
69. R. FREEMAN AND H. D. W. HILL, *J. Chem. Phys.* **54,** 301 (1971); R. FREEMAN AND H. D. W. HILL, "Dynamic Nuclear Magnetic Resonance Spectroscopy" (L. M. Jackman and F. A. Cotton, Eds.), Chap. 5, Academic Press, New York, 1975.
70. I. SOLOMON, *Compt. Rend.* **248,** 92 (1959).
71. I. SOLOMON, *Compt. Rend.* **249,** 1631 (1959).
72. J. H. STRANGE AND R. E. MORGAN, *J. Phys. C* **3,** 1997 (1970).
73. R. FREEMAN AND H. D. W. HILL, *J. Chem. Phys.* **55,** 1985 (1971).
74. R. FREEMAN, H. D. W. HILL, AND J. DADOK, *J. Chem. Phys.* **58,** 3107 (1973).
75. T. K. LEIPERT, J. H. NOGGLE, W. J. FREEMAN, AND D. L. DALRYMPLE, *J. Magn. Resonance* **19,** 208 (1975).
76. T. K. LEIPERT, W. J. FREEMAN, AND J. H. NOGGLE, *J. Chem. Phys.* **63,** 4177 (1975).
77. H. D. W. HILL, private communication.
78. P. MANSFIELD AND P. K. GRANNELL, *J. Phys. C.* **6,** L422 (1973).
79. W. S. HINSHAW, *Phys. Lett. A* **48,** 87 (1974).
80. A. N. GARROWAY, P. K. GRANNELL, AND P. MANSFIELD, *J. Phys. C* **7,** L457 (1974).
81. W. S. HINSHAW, *J. Appl. Phys.* **47,** 3709 (1975).
82. P. MANSFIELD AND P. K. GRANNELL, *Phys. Rev. B* **12,** 3618 (1975).
83. P. K. GRANNELL AND P. MANSFIELD, *Phys. Med. Biol.* **20,** 477 (1975).
84. P. MANSFIELD, A. A. MAUDSLEY, AND T. BAINES, *J. Phys. E* **9,** 271 (1976).
85. P. C. LAUTERBUR, *Nature* **242,** 190 (1973).
86. P. C. LAUTERBUR, *Pure Appl. Chem.* **40,** 149 (1974).
87. P. C. LAUTERBUR, D. M. KRAMER, W. V. HOUSE, JR., AND C.-N. CHEN, *J. Amer. Chem. Soc.* **97,** 6866 (1975).
88. A. KUMAR, D. WELTI, AND R. R. ERNST, *J. Magn. Resonance* **18,** 69 (1975).
89. R. R. ERNST, *Chimia* **29,** 179 (1975).
90. N. BLOEMBERGEN, E. M. PURCELL, AND R. V. POUND, *Phys. Rev.* **73,** 679 (1948).
91. R. FREEMAN AND B. GESTBLOM, *J. Chem. Phys.* **48,** 5008 (1968).
92. J. SCHAEFER, "Topics in Carbon-13 NMR Spectroscopy" (G. C. Levy, Ed.), Vol. 1, Chichester, Wiley–Interscience, New York, 1974.
93. M. MEHRING AND J. S. WAUGH, *Rev. Sci. Instrum.* **43,** 649 (1972).
94. F. BLOCH AND A. SIEGERT, *Phys. Rev.* **57,** 522 (1940).
95. N. F. RAMSEY, *Phys. Rev.* **100,** 1191 (1955).
96. D. ALIGHIERI, "La Divina Commedia" (G. Petrocchi, Ed.), Einaudi, Turin, 1975.
97. R. KUBO AND K. TOMITA, *J. Phys. Soc. Japan* **9,** 888 (1954).
98. C. P. SLICHTER, "Principles of Magnetic Resonance," Chap. 2, Harper & Row, New York, 1963.
99. R. R. ERNST AND W. A. ANDERSON, *Rev. Sci. Instrum.* **37,** 93 (1966).
100. E. D. OSTROFF AND J. S. WAUGH, *Phys. Rev. Lett.* **16,** 1097 (1966).
101. A. PINES AND J. D. ELLETT, JR., *J. Amer. Chem. Soc.* **95,** 4437 (1973).
102. H. Y. CARR, *Phys. Rev.* **112,** 58 (1958).
103. R. FREEMAN AND H. D. W. HILL, *J. Magn. Resonance* **4,** 366 (1971); A. SCHWENK, *J. Magn. Resonance* **5,** 376 (1971).
104. D. E. JONES AND H. STERNLICHT, *J. Magn. Resonance* **6,** 167 (1972).

105. J. KRONENBITTER AND A. SCHWENK, *J. Magn. Resonance* **25,** 147 (1977).
106. F. BLOCH, *Phys. Rev.* **70,** 460 (1946).
107. R. BRACEWELL, "The Fourier Transform and Its Applications," McGraw–Hill, New York, 1965.
108. D. S. CHAMPENEY, "Fourier Transforms and Their Physical Applications," Academic Press, New York, 1973.
109. M. HANSEN AND H. J. JAKOBSEN, *J. Magn. Resonance* **10,** 74 (1973).
110. H. C. TORREY, *Phys. Rev.* **76,** 1059 (1949).
111. F. W. DAHLQUIST, K. J. LONGMUIR, AND R. B. DUVERNET, *J. Magn. Resonance* **17,** 406 (1975).
112. A. G. REDFIELD AND R. K. GUPTA, *Cold Spring Harbor Symp. Quant. Biol.* **36,** 405 (1963).
113. B. E. MANN, *J. Magn. Resonance* **21,** 17 (1976).
114. P. AHLBERG, *Chem. Scr.* **9,** 47 (1976).
115. B. E. MANN, *J. Magn. Resonance* **25,** 91 (1977).
116. B. E. MANN, *J. Chem. Soc. Perkin II* 84 (1977).
117. R. FREEMAN AND H. D. W. HILL, *J. Chem. Phys.* **54,** 3367 (1971).
118. L. MÜLLER, A. KUMAR, AND R. R. ERNST, *J. Chem. Phys.* **63,** 5490 (1975).
119. G. BODENHAUSEN, R. FREEMAN, AND D. L. TURNER, *J. Chem. Phys.* **65,** 839 (1976).
120. G. BODENHAUSEN, R. FREEMAN, R. NIEDERMEYER, AND D. L. TURNER, *J. Magn. Resonance* **24,** 291 (1976).
121. L. MÜLLER, A. KUMAR, AND R. R. ERNST, *J. Magn. Resonance* **25,** 383 (1977).
122. G. BODENHAUSEN, R. FREEMAN, G. A. MORRIS, AND D. L. TURNER, *J. Magn. Resonance* **28,** 17 (1977).
123. J. JEENER, Ampere International Summer School II, Basko Polje, Yugoslavia, 1971; Second European International NMR Conference, Enschedé, Holland, 1975.
124. W. P. AUE, E. BARTHOLDI, AND R. R. ERNST, *J. Chem. Phys.* **64,** 2229 (1976).
125. G. BODENHAUSEN, R. FREEMAN, R. NIEDERMEYER, AND D. L. TURNER, *J. Magn. Resonance* **26,** 133 (1977).